Brittle-ductile deformation of granulitic clinopyroxene during incipient eclogitisation

Larissa Lenz[1*], Sascha Zertani[2], Bernhard Grasemann[3], Roland Stalder[4], Luca Menegon[5] and Anna Rogowitz[1]

1 - University of Innsbruck, Institute of Geology, Innsbruck, Austria 2 - Stockholm University, Department of Geological Sciences, Stockholm, Sweden 3 - University of Vienna, Department of Geology, Vienna, Austria
4 - University of Innsbruck, Institute of Mineralogy and Petrography, Innsbruck, Austria 5 - University of Oslo, Department of Geosciences, Oslo, Norway *larissa.lenz@uibk.ac.at

FWF Österreichischer Wissenschaftsfonds

universität innsbruck

EGU 26-5725

Sharing not permitted

In the mafic lower crust, clinopyroxene is among the main rock-forming minerals. Based on experimental investigations, clinopyroxene is considered to be strong and to deform in a brittle manner at dry lower crustal conditions. However, field observations on Holsnøy, Norway, indicate ductile deformation of coarse-grained clinopyroxene in the mafic lower crust, reflected by the bending of the granulitic folitation adjacent to the eclogitic shear zones (Fig. 1).

This study focusses on the strain accommodating processes of the granulitic clinopyroxene during incipient eclogitisation. Our investigations show the complex interplay of brittle and ductile processes on a microscopic scale during macroscopically ductile flow.

The study area: Holsnøy, Norway

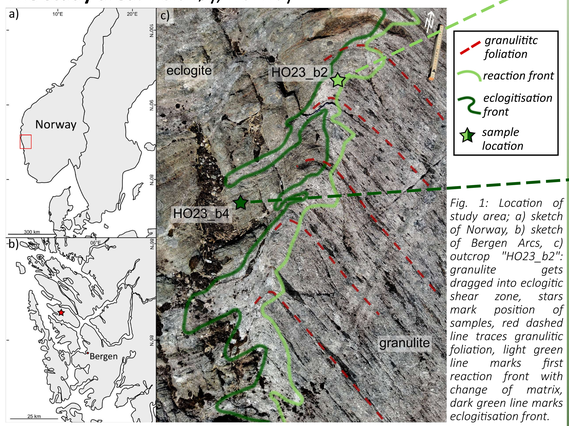


Fig. 1: Location of study area; a) sketch of Norway, b) sketch of Bergen Arcs, c) outcrop "HO23_b2": granulite gets dragged into eclogitic shear zone, stars mark position of samples, red dashed line traces granulitic foliation, light green line marks first reaction front with change of matrix, dark green line marks eclogitisation front.

Petrological observations

Granulitic sample



- matrix of plagioclase (**Plg**) and (clino-)zoisite (**Czo**)
- garnet grains mainly in matrix (**Grt$_M$**)
- bent aggregates of clinopyroxene grains (**Di I**)

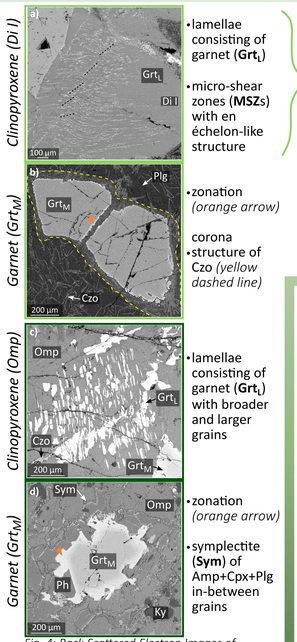
Fig. 2: Thin section scan of granulitic sample "HO23_b2".

Eclogitic sample



- matrix of omphacite (**Omp**), clinozoisite (**Czo**), kyanite (**Ky**) and minor quartz (**Qz**) and phengite (**Ph**)
- garnet grains in matrix (**Grt$_M$**) with corona (Omp, Qz, Ky, Ph)
- large aggregates of Omp with relict Di I grains *(green dashed line)*

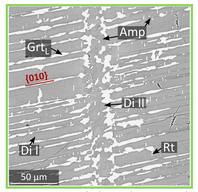
Fig. 3: Thin section scan of eclogitic sample "HO23_b4".



- lamellae consisting of garnet (**Grt$_L$**)
- micro-shear zones (**MSZs**) with en échelon-like structure
- zonation *(orange arrow)*
- corona structure of Czo *(yellow dashed line)*
- lamellae consisting of garnet (**Grt$_L$**) with broader and larger grains
- zonation *(orange arrow)*
- symplectite (**Sym**) of Amp+Cpx+Plg in-between grains

Fig. 4: Back-Scattered Electron Images of "HO23_b2" (a,b) & "HO23_b4" (c,d).

Micro-Shear Zone



- lamellar Grt$_L$ and amphibole (**Amp**) parallel to {010}$_{Di\ I}$
- new phases at micro-shear zones (**MSZs**): **Grt$_L$**, **Amp**, **Di II**, minor rutile (**Rt**)

Fig. 5: Detailed Back-Scattered Electron image of a micro-shear zone in Di I.

Quantitative composition

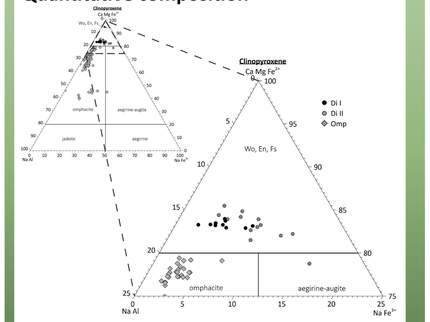
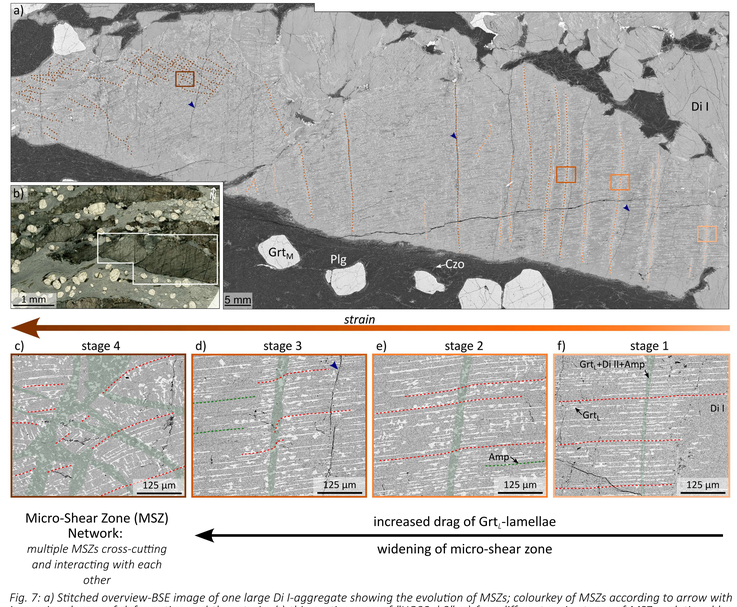


Fig. 6: Compositional classification of clinopyroxene of granulitic sample (Di I & Di II) and eclogitic sample (Omp).

Microstructural evolution of micro-shear zones



Micro-Shear Zone (MSZ) Network:
multiple MSZs cross-cutting and interacting with each other

increased drag of Grt$_L$-lamellae

widening of micro-shear zone

Fig. 7: a) Stitched overview-BSE image of one large Di I-aggregate showing the evolution of MSZs; colourkey of MSZs according to arrow with increasing degree of deformation and thus strain; b) thin section scan of "HO23_b2"; c) four different main stages of MSZ evolution; blue arrow indicates retrograde cracks.

Chemical & crystallographic evolution of micro-shear zones

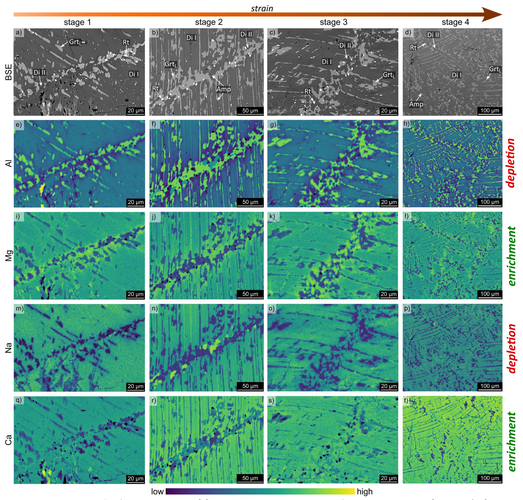
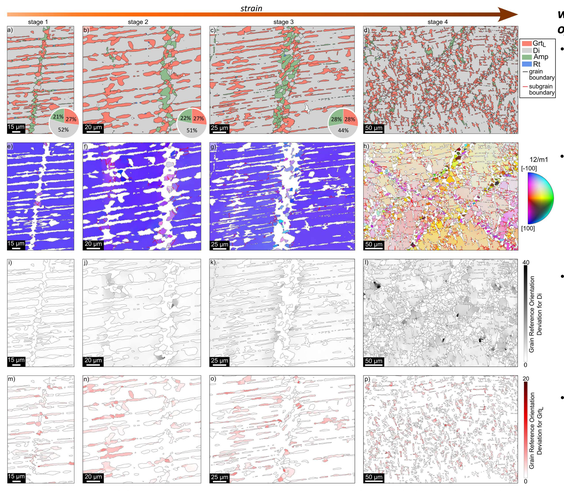


Fig. 8: BSE images & element maps of four MSZ-stages; arrow indicates increase of strain (c.f. Fig. 7); colour scheme of element maps with blue = low content, yellow = high content; for all stages enrichment of Mg & Ca, depletion of Al & Na towards MSZ.

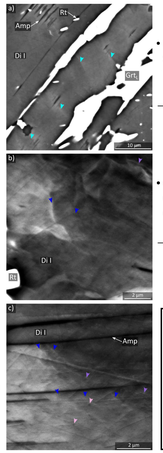


with increase of strain:

- higher content of Amp & Grt$_L$ in MSZ
- higher variance in orientation of Di II compared to Di I
- higher mis-orientation in Di I towards MSZ
- higher mis-orientation in lamellar Grt$_L$ compared to Grt$_L$ in MSZ

Fig. 9: EBSD maps of four MSZ-stages; arrow indicates increase of strain (c.f. Fig. 7); a-d) phase maps, pie chart shows content of phases in MSZ; e-h) orientation of diopsidic clinopyroxene (Di I & Di II) overlain by subgrain boundaries (red); i-p) misorientation to mean orientation of Di I & Di II (i-l), and of Grt$_L$ (m-p).

Origin of subgrains in Di I:



- micro-fracturing sub-perpendicular to lamellae of Grt$_L$

→ ***micro-cracks***

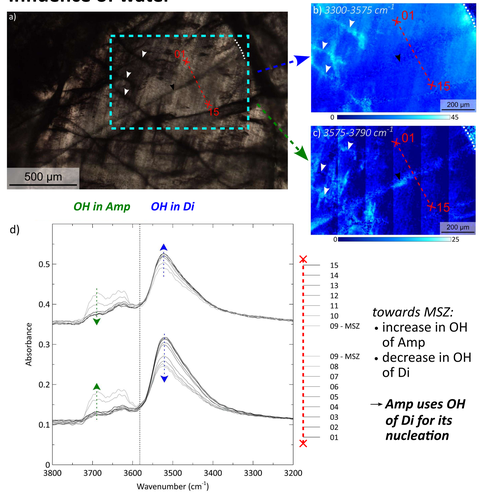
- crystal lattice distortion & dislocations

→ ***crystal-plasticity***

- *micro-cracks*
- *crystal lattice distortion*
- *shallow or steep inclined dislocations to sample surface*

Fig. 10: Electron Channeling Contrast images of Di I showing brittle and ductile deformation at nano scale.

Influence of water



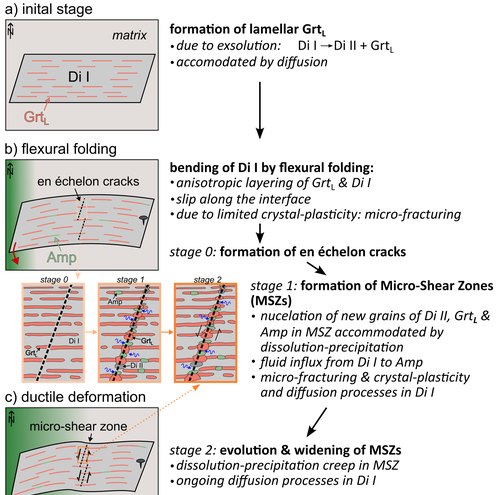
towards MSZ:

- increase in OH of Amp
- decrease in OH of Di

→ ***Amp uses OH of Di for its nucleation***

Fig. 11: Fourier-Transform Infrared Spectroscopy of granulitic clinopyroxene; a) location of FTIR-Imaging and profile; b) FTIR-Imaging for Di at 3300-3575 cm^{-1}; c) FTIR-Imaging for Amp at 3575-3700 cm^{-1}; d) profile across a Micro-Shear Zone (MSZ; black arrow); white arrows indicate late cracks with free water.

Interplay of brittle & ductile deformation



formation of lamellar Grt$_L$
- *due to exsolution:* Di I → Di II + Grt$_L$
- *accomodated by diffusion*

bending of Di I by flexural folding:
- *anisotropic layering of Grt$_L$ & Di I*
- *slip along the interface*
- *due to limited crystal-plasticity: micro-fracturing*

stage 0: **formation of en échelon cracks**

stage 1: **formation of Micro-Shear Zones (MSZs)**
- *nucelation of new grains of Di II, Grt$_L$ & Amp in MSZ accommodated by dissolution-precipitation*
- *fluid influx from Di I to Amp*
- *micro-fracturing & crystal-plasticity and diffusion processes in Di I*

stage 2: **evolution & widening of MSZs**
- *dissolution-precipitation creep in MSZ*
- *ongoing diffusion processes in Di I*

Fig. 12: Sketch of different deformation stages of granulitic clinopyroxene during incipient eclogitisation.